Exact effective transport dynamics in a one-dimensional random environment

Marco Dentz*
Department of Geotechnical Engineering and Geosciences, Technical University of Catalonia (UPC), Barcelona, Spain

Brian Berkowitz†
Department of Environmental Sciences and Energy Research, Weizmann Institute of Science, Rehovot, Israel
(Received 12 April 2005; revised manuscript received 7 June 2005; published 28 September 2005)

We study effective transport under linear equilibrium adsorption characterized by a spatially random retardation factor. In a stochastic framework, we present a methodology to quantify explicitly the impact of spatial disorder on effective transport dynamics. We derive an exact effective transport equation, which is equivalent to transport under linear kinetic adsorption characterized by a spectrum of adsorption times. The distribution of adsorption times is given explicitly in terms of the spatial disorder distribution. Furthermore, we find that effective transport is formally equivalent to a decoupled continuous time random walk. This observation and the explicit nature of the presented results allow for a mapping of the static disorder distribution on the transition time distribution.

DOI: 10.1103/PhysRevE.72.031110 PACS number(s): 05.40.Fb, 05.60.−k, 02.50.−r

I. INTRODUCTION

Transport in heterogeneous media can be dramatically different from transport in a homogeneous environment, as the impact of spatial heterogeneities leads in general to different effective transport dynamics. We consider here a model that describes one-dimensional transport with spatially random equilibrium adsorption. Transport under linear adsorption reactions finds application in many fields ranging from the modeling of chromatographic systems (e.g., [1,2]), to description of reactive contaminant transport (e.g., [3–6]), to treatment of transport processes in biological systems (e.g., [7–11]). For biological applications, the understanding of transport under sorption-desorption reactions is important for modeling protein movements and infection pathways of viruses, for example. In the context of hydrology, sorption-desorption reactions play a key role in the transport of many natural and anthropogenic contaminants such as organic compounds, heavy and transition metals, and radionuclides.

In such systems the transported particles can be immobilized by sorption to the matrix of the transport medium and mobilized again by desorption. Thus the total solute or particle distribution $c(x,t)$ is divided into a mobile fraction $c_m(x,t)$ and an adsorbed fraction $c_{ad}(x,t)$,

$$c(x,t) = c_m(x,t) + c_{ad}(x,t). \tag{1}$$

Transport in the mobile phase is given by advection driven by a potential gradient, and molecular diffusion or dispersion. We consider here linear sorption processes for which the typical sorption time scale is small compared to a typical advection time scale, i.e., equilibrium between the mobile and immobile phases can be considered as instantaneous. The adsorbed and mobile distributions are then related by

$$c_{ad}(x,t) = k_d(x)c_m(x,t) \tag{2}$$

with a distribution coefficient $k_d(x) \geqslant 0$ that varies in space as a consequence of chemical heterogeneities of the underlying transport medium. In geological formations and soil columns, for example, such heterogeneities originate from the composition of the medium of materials with different adsorption properties. The total and mobile particle distributions are related by

$$c(x,t) = \theta(x)c_m(x,t), \tag{3}$$

where the random retardation factor is defined by

$$\theta(x) \equiv 1 + k_d(x) \geqslant 1. \tag{4}$$

We investigate here the impact of spatial fluctuations of $\theta(x)$ on effective transport dynamics.

The characterization of transport in random environments has been studied frequently in the literature in the context of transport in turbulent and static random flow fields as well as for the random adsorption problem under consideration here (e.g., [5,6,12–26]). Frequently, transport has been characterized by effective transport coefficients such as effective retardation (e.g., [27,28]) and effective dispersion coefficients (e.g., [19,21]), for example. Such effective transport coefficients are in general time dependent, which indicates transport dynamics different from those for a homogeneous environment.

The derivation of effective transport dynamics involves averaging of the equation describing transport in the random medium over the ensemble of all realizations of the underlying random fields. This leads to effective equations which are characterized by spatial and temporal memory terms (e.g, [13,20,23,26,29–33]). Due to the complexity of the underlying transport problems such studies are often limited to perturbation theory, which is, however, insufficient for a consistent effective transport description (e.g., [23,30]). In the context of nonequilibrium transport and irreversible thermodynamics, effective transport coefficients have been ex-

*Electronic address: marco.dentz@upc.es
†Electronic address: brian.berkowitz@weizmann.ac.il

pressed as integrals of time-correlation functions (e.g., [34–37]), which are related to memory kernels in effective transport equations (e.g., [38]). The latter studies deal with the influence of thermal fluctuations on effective transport behavior, while here we focus on the impact of static spatial fluctuations.

Continuous time random walk (CTRW) theory (e.g., [39–44]) represents a nonperturbative effective framework to model transport in heterogeneous environments. In this approach, the impact of medium heterogeneities on effective transport is modeled by a joint transition length and time distribution. The effective transport equation is characterized by a temporal memory term, which is a functional of the transition time distribution. The latter is frequently modeled on the basis of phenomenological considerations and an exact map of the disorder distribution onto the transition time distribution is often not known. In the physics literature, CTRW has been used to model charge and energy transport in dielectric and semiconducting material, e.g., [40–42,45–47]. For such systems, Klafter and Silbey [48] derived a CTRW equation by performing a formal ensemble average. In hydrology CTRW has been used to model and understand anomalous contaminant transport in heterogeneous geological formations, e.g., [43,49–54]. If the joint transition length and time distribution can be decoupled, CTRW encompasses multitrapping and linear multirate mass transfer (MRMT) (e.g., [45,53,55]). MRMT models (e.g., [45,47,56–59]) have been used to describe trap-controlled photoconduction (e.g., [45,60]), to model chromatographic systems (e.g., [1]) as well as to describe solute transport in soil physics and hydrology (e.g., [4,57]).

In the following, we develop a methodology to systematically incorporate spatial fluctuations of the linear adsorption properties into an effective transport picture. We derive an exact nonperturbative effective transport framework, which is characterized by a temporal memory kernel. The latter is explicitly related to the heterogeneity distribution. We show that transport under spatially heterogeneous equilibrium adsorption reactions is equivalent to transport with kinetic linear adsorption for sufficiently large time and length scales. Furthermore, we find that the derived effective transport dynamics are formally equivalent to a decoupled CTRW, which delivers an explicit expression for the transition time distribution in terms of the disorder distribution.

II. TRANSPORT MODEL

We consider advective-diffusive transport of a scalar $c(x,t)$ in a one-dimensional chemically heterogeneous environment under linear instantaneous equilibrium adsorption. The temporal change of $c(x,t)$ is balanced by the divergence of the advective and diffusive fluxes of the nonadsorbed mobile fraction $c_m(x,t)$ and reads as

$$\frac{\partial}{\partial t}c(x,t) + \left\{ q\frac{\partial}{\partial x} - \mathcal{D}\frac{\partial^2}{\partial x^2} \right\} c_m(x,t) = 0, \tag{5}$$

where q denotes the constant drift and $\mathcal{D}$ the (constant) molecular diffusion coefficient. Equation (5) is closed by relation (3) between the total and mobile distributions. Using (3) in (5), we obtain for the temporal evolution of $c_m(x,t)$,

$$\theta(x)\frac{\partial}{\partial t}c_m(x,t) + \left\{ q\frac{\partial}{\partial x} - \mathcal{D}\frac{\partial^2}{\partial x^2} \right\} c_m(x,t) = 0. \tag{6}$$

Substituting $c_m(x,t) = \theta(x)^{-1}c(x,t)$ into (5), we obtain for the total particle distribution the Fokker-Planck equation

$$\frac{\partial}{\partial t}c(x,t) + \left\{ \frac{\partial}{\partial x}\frac{q}{\theta(x)} - \frac{\partial^2}{\partial x^2}\frac{\mathcal{D}}{\theta(x)} \right\} c(x,t) = 0, \tag{7}$$

with spatially varying drift and diffusion coefficients. As boundary conditions we assume a vanishing $c(x,t)$ at $x = \pm\infty$; the initial condition is $c(x,t=0) = \delta(x)$. The initial and boundary conditions for $c_m(x,t)$ follow from relation (3).

For completeness, we note that the Langevin equation associated with the Fokker-Planck equation (7) reads in the Ito interpretation as (e.g., [61])

$$\frac{d}{dt}x(t) = \frac{q}{\theta(x(t))} + \frac{\xi(t)}{\sqrt{\theta(x(t))}}, \tag{8}$$

where $\xi(t)$ is a white Gaussian noise with zero mean and correlation:

$$\langle \xi(t)\xi(t') \rangle = 2\mathcal{D}\delta(t-t'). \tag{9}$$

The angular brackets denote the average over the white noise realizations. Transport under random adsorption conditions describes a continuum random walk with spatially random drift and diffusion coefficients. Because of equilibrium sorption-desorption reactions, the movement and spreading of the particles is retarded, which is reflected by the reduced drift and diffusion coefficients.

The impact of the spatial fluctuations of the retardation factor $\theta(x)$ on effective transport is addressed in a stochastic modeling framework, in which the retardation factor $\theta(x)$ is modeled as a translation invariant random field. Translational invariance implies that

$$\overline{\theta(x)} = 1 + \overline{k_d(x)} \tag{10}$$

is constant, where the overbar in the following denotes the ensemble average. We decompose $\theta(x)$ as

$$\theta(x) = \bar{\theta}(1 + r(x)), \tag{11}$$

with the mean $\overline{r(x)} \equiv 0$ by definition. The random field $r(x)$ is characterized completely by its distribution functional $\mathcal{P}(\{r(x)\})$. In the following we do not need to make an explicit assumption on the distribution of $r(x)$ except that it is restricted to $r(x) \geqslant -r_0$ with

$$r_0 = \frac{\bar{\theta} - 1}{\bar{\theta}} > 0 \tag{12}$$

as a consequence of (4).

We rescale the mobile particle fraction, the drift and diffusion coefficients in the mobile phase by the average retardation factor $\bar{\theta}$ according to

$$g(x,t) = \bar{\theta} c_m(x,t), \quad u = q/\bar{\theta}, \quad D = \mathcal{D}/\bar{\theta}. \tag{13}$$

Inserting these definitions into (6) we obtain for $g(x,t)$,

$$\frac{\partial}{\partial t} g(x,t) + u \frac{\partial}{\partial x} g(x,t) - D \frac{\partial^2}{\partial x^2} g(x,t) = -r(x) \frac{\partial}{\partial t} g(x,t). \tag{14}$$

The total distribution (3) reads in terms of $g(x,t)$ as

$$c(x,t) = (1 + r(x)) g(x,t). \tag{15}$$

III. ENSEMBLE AVERAGE

In this section, we derive an effective transport framework by performing an ensemble average of the transport equation (14) over the spatial random field $r(x)$. We first outline the general methodology to perform the ensemble average over (14). This leads to formal effective transport equations for the Fourier-Laplace transforms of the total and mobile particle distributions in terms of the "self-energy," a quantity which integrates the influence of spatial heterogeneity on effective transport. For a short-range correlated random retardation factor, we then derive an exact nonperturbative expression for the self-energy, which defines an explicit effective transport framework.

A. General methodology

For technical convenience, we formulate the transport equation (14) as an integral equation in Fourier-Laplace space. Fourier and Laplace transforms are defined in Appendix A. Fourier transformed quantities in the following are marked by a tilde, Laplace transformed quantities by an asterisk. Furthermore, we employ the short-hand notation

$$\int_{k'} \cdots \equiv \int \frac{dk'}{(2\pi)^d} \cdots . \tag{16}$$

Fourier-Laplace transform of (14) yields

$$s\tilde{g}^*(k,s) - \{iuk - kDk\}\tilde{g}^*(k,s) = 1 - s \int_{k'} \tilde{r}(k') \tilde{g}^*(k-k',s). \tag{17}$$

From (17), we obtain the integral equation

$$\tilde{g}^*(k,s) = \tilde{g}_0^*(k,s) - s\tilde{g}_0^*(k,s) \int_{k'} \tilde{r}(k') \tilde{g}^*(k-k',s), \tag{18}$$

where the "bare" solution $\tilde{g}_0^*(k,s)$ is given by

$$\tilde{g}_0^*(k,s) = \frac{1}{s - iuk + kDk} \tag{19}$$

and solves (17) for $\tilde{r}(k) \equiv 0$.

We seek an effective equation for the ensemble average of $\overline{\tilde{g}^*}(k,s) \equiv \overline{\tilde{g}^*(k,s)}$. As a first step, we consider the ensemble average of the integral equation (18),

$$\overline{\tilde{g}^*}(k,s) = \tilde{g}_0^*(k,s) - \tilde{g}_0^*(k,s) \int_{k'} \overline{\tilde{r}(k') \tilde{g}^*(k-k',s)}. \tag{20}$$

Using the translational invariance of $r(x)$, we derive from (20),

$$\overline{\tilde{g}^*}(k,s) = \tilde{g}_0^*(k,s) + [\tilde{g}_0^*(k,s)]^2 \times s^2 \int_{k'} \int_{k''} \overline{\tilde{r}(k') \tilde{r}(k'') \tilde{g}^*(k-k',s)} \tag{21}$$

as outlined in Appendix B. Equations (20) and (21) are not closed with respect to $\overline{\tilde{g}^*}(k,s)$. We define now the self-energy $\Sigma(k,s)$ by expressing $\overline{\tilde{g}^*}(k,s)$ as

$$\overline{\tilde{g}^*}(k,s) \equiv \{s - iuk + kDk - \Sigma(k,s)\}^{-1}. \tag{22}$$

Rewriting (22) implies in fact an effective transport equation for $\overline{\tilde{g}^*}(k,s)$,

$$s\overline{\tilde{g}^*}(k,s) - \Sigma(k,s)\overline{\tilde{g}^*}(k,s) = 1 - \{iuk - kDk\}\overline{\tilde{g}^*}(k,s), \tag{23}$$

which, however, is only formal at this point because it depends on the unknown self-energy $\Sigma(k,s)$.

By comparison of (21) and (22), we can express $\Sigma(k,s)$ as

$$\Sigma(k,s) = \frac{\tilde{\Phi}(k,s)}{1 + \tilde{g}_0^*(k,s)\tilde{\Phi}(k,s)}, \tag{24}$$

where we defined

$$\tilde{\Phi}(k,s) \equiv s^2 \int_{k'} \int_{k''} \overline{\tilde{r}(k') \tilde{r}(k'') \tilde{g}^*(k-k',s)}. \tag{25}$$

Equation (23) represents an effective equation for the rescaled mobile distribution. We derive now a corresponding equation for the total average distribution $\overline{\tilde{c}^*}(k,s) \equiv \overline{\tilde{c}^*(k,s)}$. By Fourier-Laplace transform of (15), we obtain

$$\overline{\tilde{c}^*}(k,s) = \overline{\tilde{g}^*}(k,s) + \int_{k'} \overline{\tilde{r}(k') \tilde{g}^*(k-k',s)}. \tag{26}$$

Solving (20) for the second term on the right of (26) and using definition (19) of the bare propagator and definition (22) of $\Sigma(k,s)$, we obtain

$$\int_{k'} \overline{\tilde{r}(k') \tilde{g}^*(k-k',s)} = -s^{-1}\Sigma(k,s)\overline{\tilde{g}^*}(k,s). \tag{27}$$

Inserting (27) in (26), we obtain

$$\overline{\tilde{c}^*}(k,s) = \{1 - s^{-1}\Sigma(k,s)\}\overline{\tilde{g}^*}(k,s). \tag{28}$$

Combining (23) and (28), we obtain a formal effective equation for the average total distribution

$$s\overline{\tilde{c}^*}(k,s) - \{iuk - kDk\}\{1 - s^{-1}\Sigma(k,s)\}^{-1}\overline{\tilde{c}^*}(k,s) = 1. \tag{29}$$

The effective equations (23) and (29) for the mobile and total distributions, respectively, are merely formal as long as the self-energy $\Sigma(k,s)$ is not known. The self-energy integrates the impact of spatial heterogeneity on effective transport. In the following, we derive an explicit nonperturbative expression for $\Sigma(k,s)$, which renders an explicit effective

transport description. To this end, we consider a short-range correlated random retardation factor $r(x)$. The distribution of the short-range correlated $r(x)$ is specified in the following subsection.

B. Heterogeneity distribution

The normalized fluctuations $r(x)$ of the random retardation factor are modeled as a short range correlated random field, characterized by the correlation scale l. On the observation scale $L \gg l, r(x)$ can then be considered delta correlated, i.e., two random variables $r(x^{(i)})$ and $r(x^{(j)})$ are identically distributed and statistically independent for $x^{(i)} \neq x^{(j)}$. Thus the random field $r(x)$ is characterized by the single variable distribution $P(r)$ with $P(r)dr$ being the probability to find, at any given position x, a value for r in the interval $[r, r+dr]$. The moments of $P(r)$ are defined by

$$m_r^{(j)} \equiv \int_{-r_0}^{\infty} dr\, P(r) r^j, \tag{30}$$

where $m_r^{(1)} \equiv 0$ because $\overline{r(x)} \equiv 0$.

The n-point joint probability distribution of the uncorrelated random field $r(x)$ is given in terms of the single variable distribution $P(r)$ and reads as

$$\mathcal{P}(\{r(x^{(i)})\}_{i=1}^n) = \exp\left[\sum_{i=1}^{n} \ln\{P(r(x^{(i)}))\}\right]. \tag{31}$$

The 2-point correlation function is then given by

$$C_2^{ij} \equiv C_2(x^{(i)}, x^{(j)}) \equiv \overline{r(x^{(i)}) r(x^{(j)})} = m_r^{(2)} l \delta(x^{(i)} - x^{(j)}). \tag{32}$$

Note that two $r(x^{(i)})$ and $r(x^{(j)})$ are correlated only if they are at the same location, i.e., $x^{(i)} = x^{(j)}$, which is reflected by the delta distribution in (32). The N-point correlation function $\langle r(x^{(1)}) \ldots r(x^{(N)}) \rangle$ is the sum of the contribution

$$C_N^{1\ldots N} \equiv C_N(x^{(1)}, \ldots, x^{(N)}) \equiv m_r^{(N)} l^{N-1} \delta(x^{(1)} - x^{(2)}) \times \cdots \times \delta(x^{(N-1)} - x^{(N)}), \tag{33}$$

which requires $x^{(1)} = \cdots = x^{(N)}$ as expressed by the delta distributions, and all other combinations of possible averages, which require that at least two positions $x^{(i)}, x^{(j)}$ are different from all other $x^{(k)}$. For $N=4$, the average reads as

$$\overline{r(x^{(1)}) \ldots r(x^{(4)})} = C_4^{1234} + C_2^{12} C_2^{34}|_{x_1 \neq x_4} + C_2^{13} C_2^{24}|_{x_1 \neq x_2} + C_2^{14} C_2^{23}|_{x_1 \neq x_3}. \tag{34}$$

The subscripts for the second to fourth terms on the right side indicate the requirement that at least two positions are different from all the others. For the second expression on the right this means $x_1 \neq x_4$ and by the definitions (32) and (33) this implies that $x_1 = x_2 \neq x_4$ and $x_1 = x_2 \neq x_3$. Note that $C_1(x) \equiv 0$ because $\overline{r(x)} \equiv 0$ by definition. The Fourier transform of (33) is given by

$$\tilde{C}_N(k^{(1)}, \ldots, k^{(N)}) = m_r^{(N)} l^{N-1} 2\pi \delta(k^{(1)} + \cdots + k^{(N)}). \tag{35}$$

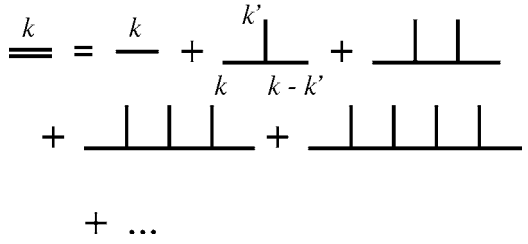

FIG. 1. Diagrammatic representation of the perturbation expansion (36) for $\tilde{g}^*(k,s)$.

C. Exact closed form expression for the self-energy

Having defined the distribution of the random field $r(x)$, we can now perform explicitly the ensemble averages involved in the calculation of the self-energy $\Sigma(k,s)$ as outlined in Sec. III A.

By iteration of the integral equation (18), we obtain a perturbation series for $\tilde{g}^*(k,s)$,

$$\tilde{g}^*(k,s) = \tilde{g}_0^*(k,s) + \sum_{n=1}^{\infty} \tilde{g}_n^*(k,s) \tag{36}$$

with

$$\tilde{g}_n^*(k,s) = (-1)^n s^n \tilde{g}_0^*(k,s) \times \int_{k^{(1)}} \cdots \int_{k^{(n)}} \tilde{r}(k^{(1)}) \tilde{g}_0^*(k - k^{(1)}, s) \tilde{r}(k^{(2)}) \times \cdots \times \tilde{r}(k^{(n)}) \tilde{g}_0(k - k^{(1)} - \cdots - k^{(n)}, s). \tag{37}$$

The first five terms of the perturbation series (36) are illustrated in diagrammatic form in Fig. 1. The horizontal double line represents $\tilde{g}^*(k,s)$, a single horizontal line $\tilde{g}_0^*(k,s)$. The vertical lines represent a $\tilde{r}(k)$. The functions associated in this manner are taken at the wave vectors indicated at the respective lines. The wave vectors at the horizontal and vertical lines sum up from right to left to the value on the left side. Thus the wave vectors in a diagram are given uniquely by the wave vector on the left and therefore will be omitted in the following. A vertex of horizontal and vertical lines is associated with a factor $-s$. Diagrams containing horizontal and vertical lines are integrated over the primed wave vectors.

Averaging over (36), gives a series expansion for $\bar{\tilde{g}}(k,s)$,

$$\overline{\tilde{g}^*}(k,s) = \tilde{g}_0^*(k,s) + \sum_{n=2}^{\infty} \overline{\tilde{g}^*}_n(k,s) \tag{38}$$

with the $\overline{\tilde{g}^*}_n(k,s)$ defined by

$$\overline{\tilde{g}_n^*}(k,s) = (-1)^n s^n [\tilde{g}_0^*(k,s)]^2 \int_{k^{(1)}} \cdots \int_{k^{(n)}} \tilde{g}_0^*(k - k^{(1)}, s) \times \cdots \times \tilde{g}_0(k - k^{(1)} - \cdots - k^{(n-1)}, s) \times \overline{\tilde{r}(k^{(1)}) \times \cdots \times \tilde{r}(k^{(n)})}. \tag{39}$$

The average (39) can be represented in diagrammatic form. Figure 2 shows the diagrammatic representation for the fourth-order contribution $\overline{\tilde{g}_4^*}(k,s)$. The average is performed

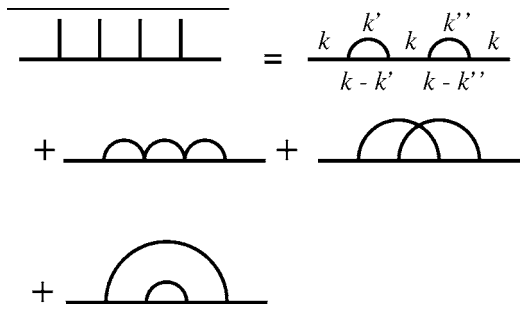

FIG. 2. Diagrammatic representation of the fourth-order contribution to $\tilde{g}^*(k,s)$ for an uncorrelated random field $r(x)$ in $d=1$ dimension.

by connecting vertices in the following way. At every vertex one has at most one in-coming and one outgoing r-line, while incoming lines come from the left and outgoing lines go to the right. Two connected vertices are associated to $\tilde{C}_2(k^{(1)},k^{(2)})$, three connected vertices to $\tilde{C}_3(k^{(1)},k^{(2)},k^{(3)})$, and so on. The average (39) then is given in diagrammatic form by the sum of all possible diagrams that can be constructed in this way. Figure 2 reflects expression (34) for the four-point correlation function. The sum of the wave numbers at every vertex is zero, while the wave number of an outgoing line is subtracted, the wave number of an incoming line is added. Finally, the inner wave numbers are integrated over.

Inserting the series expansion (36) into (25) yields for $\tilde{\Phi}(k,s)$,

$$\tilde{\Phi}(k,s) = \sum_{n=2}^{\infty} \tilde{\Phi}_n(k,s) \tag{40}$$

with the $\tilde{\Phi}_n(k,s)$ being given by

$$\begin{aligned}\tilde{\Phi}_n(k,s) = (-1)^n s^n \int_{k^{(1)}} \cdots \int_{k^{(n)}} \tilde{g}_0^*(k-k^{(1)},s)\cdots \\ \times \tilde{g}_0^*(k-k^{(1)}-\cdots-k^{(n-1)},s) \\ \times \overline{\tilde{r}(k^{(1)})\times\cdots\times\tilde{r}(k^{(n)})}.\end{aligned} \tag{41}$$

The fourth-order contribution $\tilde{\Phi}_4(k,s)$ is illustrated diagrammatically in Fig. 3. The external lines are cut, which corresponds to a division by $[\tilde{g}_0^*(k,s)]^2$ of the corresponding expressions contributing to $\tilde{g}^*(k,s)$; compare (39) and (41).

In order to obtain a corresponding series expansion for $\Sigma(k,s)$, we insert expansion (40) into (24) for $\Sigma(k,s)$ and

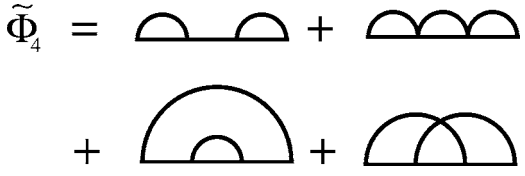

FIG. 3. Diagrammatic representation of the fourth-order contribution to $\tilde{\Phi}(k,s)$ for an uncorrelated random field $r(x)$ in $d=1$ dimension.

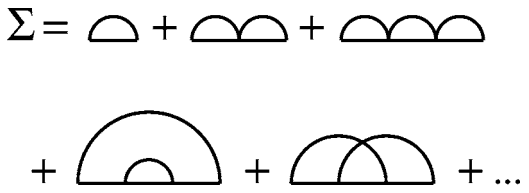

FIG. 4. Diagrammatic representation of the terms contributing to the self-energy for an uncorrelated random field $\tilde{r}(k)$ in $d=1$ dimension.

expand the denominator into a geometrical series. This yields for $\Sigma(k,s)$ in $d=1$ dimension,

$$\begin{aligned}\Sigma(k,s) &= \sum_{n=2}^{\infty} \tilde{\Phi}_n(k,s) + \sum_{i=2}^{\infty} \tilde{\Phi}_i(k,s) \sum_{j=1}^{\infty} (-1)^j \tilde{g}_0^*(k,s) \\ &\quad \times \left[\sum_{i=2}^{\infty} \tilde{\Phi}_i(k,s)\right]^j \\ &\equiv \sum_{n=2}^{\infty} \Sigma_n(k,s).\end{aligned} \tag{42}$$

Thus $\Sigma_n(k,s)$ is given by $\tilde{\Phi}_n(k,s)$ minus all possible contributions to $\tilde{\Phi}_n(k,s)$ that contain at least one "external" propagator $\tilde{g}_0^*(k,s)$. The latter contributions correspond to reducible diagrams, i.e., diagrams that can be separated into two by cutting one line. In fourth order, for example, the first diagram on the right side in Fig. 3 is reducible. Thus the self-energy $\Sigma(k,s)$ can be represented by the diagrammatic expansion illustrated in Fig. 4.

For illustration and technical convenience, we transform (41) for $\tilde{\Phi}_n(k,s)$ back to real space, which yields

$$\begin{aligned}\Phi_n(x,s) = (-1)^n s^n \int dx^{(1)} \cdots \int dx^{(n-2)} g_0^*(x-x^{(1)},s)\cdots \\ \times g_0^*(x^{(n-3)}-x^{(n-2)},s) g_0^*(x^{(n-2)},s) \\ \times \overline{r(x) r(x^{(1)}) \cdots r(x^{(n-2)}) r(0)},\end{aligned} \tag{43}$$

where $g_0^*(x,s)$, is given by

$$g_0^*(x,s) = \frac{1}{u}\exp\left(-\frac{xs}{u}\right) T(x,s), \tag{44}$$

with the function $T(x,s)$,

$$T(x,s) = \frac{1}{\sqrt{1+4\epsilon s\tau_u}} \exp\left\{-\frac{1}{2\epsilon l}\left(\sqrt{x^2+4\epsilon x^2 s\tau_u} - x - 2\epsilon x s\tau_u\right)\right\}. \tag{45}$$

We defined the inverse Peclet number $\epsilon \equiv D/ul$ and the advection time scale $\tau_u \equiv l/u$. The inverse Peclet number measures the relative importance of advective and diffusive transport over one correlation length of the medium. We focus here on advection-dominated transport, which implies $\epsilon < 1$. The advection time scale characterizes the typical time for a "transition" over one correlation length by advection, and is thus the relevant time scale for the sampling of the

medium heterogeneities. For times $t \gg \tau_u$ and distances $x \gg l$, a representative part of the heterogeneity spectrum has been sampled and an effective transport description is meaningful. Thus, we focus now on times large compared to the advection time scale, i.e., $s\tau_u \ll 1$, and distances large compared to the correlation length, i.e., $x \gg l$. In this limit, the function $\theta(x,s)$ can be approximated by the Heaviside step function,

$$T(x,s) = \Theta(x), \tag{46}$$

where $\Theta(x)$ here is 0 for $x<0$ and 1 for $x \geq 0$. Thus the "bare" propagator (45) reduces to

$$g_0^*(x,s) = \frac{1}{u}\exp\left(-\frac{xs}{u}\right)\Theta(x). \tag{47}$$

Note that this limit is equivalent to the limit of small inverse Peclet numbers, $\epsilon \ll 1$.

The step function associated with the "bare" propagator (47) implies the following order of spatial arguments in (43),

$$x \geq x^{(1)} \geq x^{(2)} \geq \cdots \geq x^{(n-2)} \geq 0. \tag{48}$$

Thus only those terms of the n-point correlation function $\overline{r(x)r(x^{(1)})\ldots r(x^{(n-2)})r(0)}$ that respect this "causality" condition contribute to $\Phi_n(x,s)$. The terms that do not conform with (48) are of subleading order in the large scale limit under consideration. Thus the leading contributions to, e.g., $\Phi_4^*(x,s)$ originating from $\overline{r(x)r(x^{(1)})r(x^{(2)})r(0)}$ are

$$C_4(x,x^{(1)},x^{(2)},0) \quad \text{and} \quad C_2(x,x^{(1)})C_2(x^{(2)},0). \tag{49}$$

The contributions due to

$$C_2(x,0)C_2(x^{(1)},x^{(2)}) \quad \text{and} \quad C_2(x,x^{(2)})C_2(x^{(1)},0) \tag{50}$$

violate the "causality" condition (48) in (43) and are subleading. In terms of the diagrammatic expansion this means that if two vertices which are not neighboring each other are connected the causal order is violated and the associated diagram is subleading because of the causality relation (48). Thus, the only relevant nth order contribution to $\Phi(x,s)$ results from the diagrams for which the vertices are connected in a causal way.

Furthermore, the only contribution to $\tilde{\Phi}_n(k,s)$ originating from $\overline{\tilde{r}(k^{(1)})\ldots\tilde{r}(k^n)}$ that does not cause an external $\tilde{g}_0^*(k,s)$ and obeys the causality condition (48) is due to $\tilde{C}_n(k^{(1)},\ldots,k^{(n)})$. In other words, the only irreducible contribution to $\tilde{\Phi}_n(k,s)$ is given by the diagram, for which all vertices are connected. The self-energy is now represented in diagrammatic form by the expansion shown in Fig. 5. Evaluating the only relevant diagram in nth order yields for $\Sigma_n(k,s)$

$$\begin{aligned}\Sigma_n(k,s) &= (-1)^n s^n m_r^{(n)} l^{n-1} \int_{k^{(1)}} \cdots \int_{k^{(n-1)}} \tilde{g}_0^*(k-k^{(1)},s) \times \cdots \\ &\quad \times \tilde{g}_0^*(k-k^{(n-1)}) \\ &= (-1)^n s^n m_r^{(n)} l^{n-1} \{g_0^*(0,s)\}^{n-1}.\end{aligned} \tag{51}$$

Inserting (47) into (51), we obtain

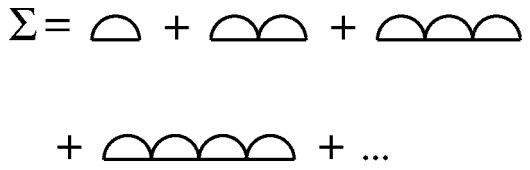

FIG. 5. Diagrammatic representation of the terms contributing to the self-energy in $d=1$ dimension for an uncorrelated random field $\tilde{r}(k)$. In the large scale limit $s\tau_u \ll 1$ and $x \gg l$, the diagrams, for which all vertices are connected in a causal way, are of leading order.

$$\Sigma_n(k,s) = \tau_u^{-1}(-1)^n (s\tau_u)^n m_r^{(n)}, \tag{52}$$

with the advection time scale $\tau_u = l/u$. Thus the self-energy $\Sigma(k,s)$ is given by the infinite series

$$\Sigma(k,s) = \tau_u^{-1} \sum_{n=2}^{\infty} (-1)^n (s\tau_u)^n m_r^{(n)}. \tag{53}$$

Using the single variable distribution $P(r)$ and the definition (30) of its moments $m_r^{(n)}$, (53) can be written as

$$\Sigma(k,s) = \tau_u^{-1} \int_{-r_0}^{\infty} dr \sum_{n=1}^{\infty} (-1)^n (rs\tau_u)^n, \tag{54}$$

where we extended the sum tautologically to include $n=1$ as $m_r^{(1)} \equiv 0$ by definition. The sum on the right side can be performed explicitly:

$$\sum_{n=1}^{\infty} (-1)^n (rs\tau_u)^n = \frac{1}{1+rs\tau_u} - 1 = \frac{-rs\tau_u}{1+rs\tau_u}. \tag{55}$$

Inserting the right side of (55) into (54) leads to the explicit expression

$$\Sigma(k,s) \equiv \Sigma(s) = -s\varphi^*(s) \tag{56}$$

for the self-energy, where we defined the memory function,

$$\varphi^*(s) \equiv \int_{-r_0}^{\infty} dr\, P(r) \frac{r}{1+rs\tau_u}. \tag{57}$$

IV. EFFECTIVE TRANSPORT

Inserting (56) into (23) and transforming the resulting equation back to real space and time, we obtain the explicit effective transport equation

$$\frac{\partial}{\partial t}\bar{g}(x,t) + \frac{\partial}{\partial t}\int_0^t dt'\, \varphi(t-t')\bar{g}(x,t') + \left\{ u\frac{\partial}{\partial x} - D\frac{\partial^2}{\partial x^2} \right\} \bar{g}(x,t) = 0 \tag{58}$$

with $\varphi(t)$ the inverse Laplace transform of (57), see Appendix C,

$$\varphi(t) = \tau_u^{-1} \int_0^{\infty} dr\, P(r) \exp\left(-\frac{t}{r\tau_u}\right). \tag{59}$$

For the total particle distribution, we obtain by inserting (56) into (29) and transformation back to real space and time,

$$\frac{\partial}{\partial t}c(x,t) + \left\{ u\frac{\partial}{\partial x} - D\frac{\partial^2}{\partial x^2} \right\} \int_0^t dt' M(t-t')c(x,t'). \quad (60)$$

The memory kernel $M(t)$ is defined by its Laplace transform as

$$M^*(s) = \{1 + \varphi^*(s)\}^{-1}. \quad (61)$$

We show in the following that the effective transport equation (58) describes transport under linear kinetic sorption-desorption reactions in an effectively homogeneous medium. Furthermore, we demonstrate that (60) describes the evolution of the total particle distribution in a continuous time random walk.

A. Transport under linear kinetic adsorption

We show here the equivalence of the effective transport dynamics given by Eq. (58) to transport under linear kinetic adsorption reactions in an effectively homogeneous medium. Substituting $\bar{g}(x,t) = \bar{\theta}\bar{c}_m(x,t)$, $u = q/\bar{\theta}$ and $D = \mathcal{D}/\bar{\theta}$, recall (13), into (58), we obtain

$$\bar{\theta}\frac{\partial}{\partial t}\bar{c}_m(x,t) + \bar{\theta}\frac{\partial}{\partial t}\int_0^t dt' \varphi(t-t')\bar{c}_m(x,t') + \left\{ q\frac{\partial}{\partial x} - \mathcal{D}\frac{\partial^2}{\partial x^2} \right\} \bar{c}_m(x,t) = 0. \quad (62)$$

We define now the (normalized) distribution of apparent adsorption times $\tau = r\tau_u$ and the adsorption rate ω by

$$P_{ad}(\tau) \equiv \left\{ \tau_u \int_0^\infty \mathrm{d}r\, P(r) \right\}^{-1} P(\tau\tau_u^{-1}) \quad (63)$$

$$\omega \equiv \tau_u^{-1} \int_0^\infty dr\, P(r), \quad (64)$$

respectively. Recall that $P(r)$ is normalized on $[-r_0, \infty[$. With these definitions, the memory function $\varphi(t)$, (59), can be rewritten as

$$\varphi(t) = \omega \int_0^\infty d\tau\, P_{ad}(\tau) \exp\left(-\frac{t}{\tau} \right). \quad (65)$$

The convolution integral in (62) defines the averaged adsorbed particle distribution $\bar{c}_{ad}(x,t)$ so that we can rewrite (62) as

$$\bar{\theta}\frac{\partial}{\partial t}\bar{c}_m(x,t) + \bar{\theta}\frac{\partial}{\partial t}\bar{c}_{ad}(x,t) + q\frac{\partial}{\partial x}\bar{c}_m(x,t) - \mathcal{D}\frac{\partial^2}{\partial x^2}\bar{c}_m(x,t) = 0. \quad (66)$$

By using (65) for $\varphi(t)$, $\bar{c}_{ad}(x,t)$ can be written as

$$\bar{c}_{ad}(x,t) = \int_0^\infty d\tau\, P_{ad}(\tau)\bar{c}_{ad}(x,t,\tau), \quad (67)$$

where we defined the distributions $\bar{c}_{ad}(x,t,\tau)$,

$$\bar{c}_{ad}(x,t,\tau) \equiv \omega \int_0^t dt' \exp\left(-\frac{t-t'}{\tau} \right) \bar{c}_m(x,t'). \quad (68)$$

The $\bar{c}_{ad}(x,t,\tau)$ solve the linear equation

$$\frac{\partial}{\partial t}\bar{c}_{ad}(x,t,\tau) = \omega\bar{c}_m(x,t) - \tau^{-1}\bar{c}_{ad}(x,t,\tau) \quad (69)$$

for the initial condition $\bar{c}_{ad}(x, t=0, \tau) = 0$.

Equations (66)–(69) describe transport under linear kinetic sorption-desorption reactions characterized by a spectrum of adsorption times τ (e.g., [57,59]), which are distributed according to (63). The average retardation factor $\bar{\theta}$ in (66) accounts for instantaneous equilibrium sorption in the mobile and kinetically adsorbed phases (e.g., [57,59]). The adsorbed particle distribution $\bar{c}_{ad}(x,t)$ is given by (67), which denotes the weighted average over the distributions $\bar{c}_{ad}(x,t,\tau)$ of particles which are adsorbed at sites characterized by the adsorption times τ. Linear kinetic sorption-desorption to a site with an adsorption time τ is expressed by Eq. (69). The apparent adsorption times are given by $\tau = r\tau_u$, i.e., they are measured in units of the advection time scale τ_u. By (rescaled) advection u a particle travels the distance of one correlation length l in the time τ_u. The adsorption time τ quantifies the additional time that it takes to travel this distance as a consequence of (the deviations from mean) adsorption. The trapping rate (64) can be written as

$$\omega = u/l_{\mathrm{free}} \quad (70)$$

with the mean free particle path l_{free} defined by the reduced correlation length l,

$$l_{\mathrm{free}} = l \Big/ \int_0^\infty dr\, P(r). \quad (71)$$

Thus we showed that the effective equation (58) describes transport under linear kinetic adsorption. This equivalence enabled us to derive the explicit expression (63) for the distribution of adsorption times $P_{ad}(\tau)$ in terms of the disorder distribution.

Note that Eqs. (66)–(69) also describe multirate mass exchange between a mobile phase and adsorbed or immobile phases, which are characterized by a spectrum of adsorption or residence times τ, e.g., [45,47,53,57–59]. While in the literature, the residence time distribution is frequently modeled on the basis of semiphenomenological considerations, relation (63) represents an explicit exact map of the heterogeneity distribution on the residence time distribution.

Furthermore, an interesting observation in Eq. (69) is that the trapping rate ω, defined by (64), is a constant and not dependent on the trapping time. In the hydrological literature it is often assumed that the trapping rate is inversely proportional to the residence time; this issue has been discussed in [53].

B. Continuous time random walks

In the following, we show that the effective dynamics given by Eq. (60) describe a decoupled CTRW,

$$x^{(N+1)} = x^{(N)} + \xi, \tag{72}$$

$$t^{(N+1)} = t^{(N)} + \tau, \tag{73}$$

characterized by the transition time distribution $\psi(t)$, which is defined by its Laplace transform as

$$\psi^*(s) = \left\{ 1 + s\tau_u + \int_0^\infty dr\, P(r) \frac{rs\tau_u}{1 + rs\tau_u} \right\}^{-1}, \tag{74}$$

and a short range transition length distribution $p(x)$ to be specified in the following. Significantly, this result provides for the first time an explicit prescription for the derivation of the transition time distribution $\psi(t)$ from an independent measurement of the heterogeneity distribution $P(r)$.

1. Equivalence to CTRW

We develop the CTRW equations for the total particle distribution $c(x,t)$ for a general joint transition length and time distribution $\psi(x,t)$. The particle distribution $P_N(x,t)$ after N steps of this space-time random walk (73) then is given by

$$P_{N+1}(x,t) = \int_0^t dt' \int d^d x' \psi(x - x', t - t') P_N(x', t'). \tag{75}$$

The frequency $R(x,t)$ for particles to just arrive at (x,t) is given by the sum over all $P_N(x,t)$,

$$R(x,t) = \sum_{N=0}^{\infty} P_N(x,t). \tag{76}$$

Thus we obtain from (75) by summation over N,

$$R(x,t) = P_0(x,t) + \int_0^t \int d^d x' \psi(x - x', t - t') R(x', t'). \tag{77}$$

The particle concentration $\bar{c}(x,t)$ at a site x at a given time t is given by the number of particles that reach x at some earlier time t' and do not make a transition to any other site x' before time t. This is expressed by

$$\bar{c}(x,t) = \int_0^t dt' \left\{ R(x,t') - \int_0^{t-t'} dt'' \psi(t'') R(x,t') \right\}, \tag{78}$$

where the transition time distribution is defined as the marginal distribution

$$\psi(t) \equiv \int d^d x' \psi(x' - x, t). \tag{79}$$

We now derive an equation for the particle distribution $\bar{c}(x,t)$. As a transport domain we consider the real axis and assume that $\bar{c}(x,t)$ vanishes at the boundaries at $x = \pm\infty$. Furthermore, we set the initial condition $P_0(x,t) = \delta(x)\delta(t)$. The Fourier-Laplace transform of (77) and (78) gives a linear system of two algebraic equations for $\tilde{R}^*(k,s)$ and $\tilde{\bar{c}}^*(k,s)$,

$$\tilde{R}^*(k,s) = 1 + \tilde{\psi}^*(k,s)\tilde{R}^*(k,s),$$

$$s\tilde{\bar{c}}(k,s) = \tilde{R}^*(k,s)[1 + \psi^*(s)]. \tag{80}$$

Solving these equations for $\overline{\tilde{c}^*}(k,s)$, we obtain

$$s\overline{\tilde{c}^*}(k,s) = 1 + \frac{s\tilde{\psi}(k,s)}{1 - \psi^*(s)} \tilde{c}^*(k,s) - \frac{s\psi^*(s)}{1 - \psi^*(s)} \overline{\tilde{c}^*}(k,s). \tag{81}$$

The spatial transitions are now assumed to be short range, i.e., $\psi(x,t)$ decreases quickly for large distances $|x|$. Thus, we approximate $\tilde{\psi}^*(k,s)$ in (81) by its Taylor expansion up to second order about $k=0$ as

$$\tilde{\psi}(k,s) = \psi^*(s) + iu^*(s)k - kD^*(s)k, \tag{82}$$

where we defined

$$u^*(s) \equiv -i \frac{\partial}{\partial k} \tilde{\psi}^*(k,s)_{k=0}, \tag{83}$$

$$D^*_{ij}(s) \equiv -\frac{1}{2} \frac{\partial^2}{\partial k_i k_j} \tilde{\psi}^*(k,s)_{k=0}. \tag{84}$$

Without loss of generality the first spatial moment of $\psi(x,t)$ is aligned with the one-direction of the coordinate system.

By inserting (82) into (81), we obtain for the total concentration distribution,

$$s\overline{\tilde{c}^*}(k,s) - \{iu^*(s)k - kD^*(s)k\} \frac{s\overline{\tilde{c}^*}(k,s)}{1 - \psi^*(s)} = 1. \tag{85}$$

The structure of this effective transport equation is of a more general nature than (60), which we obtain here from the exact derivation of effective transport.

We consider now a decoupled $\psi(x,t)$

$$\psi(x,t) = p(x)\psi(t), \tag{86}$$

where $p(x)$ is the spatial transition distribution density and reflects the advective-diffusive transport dynamics in the mobile phase. The transition time distribution density $\psi(t)$ accounts for the impact of heterogeneity on effective transport. The definitions (83) and (84) decouple accordingly,

$$u^*(s) = u\tau_0\psi^*(s), \tag{87}$$

$$D^*_{ij}(s) = D_{ij}\tau_0\psi^*(s), \tag{88}$$

where we defined

$$u \equiv -i\tau_0^{-1} \frac{\partial}{\partial k} \tilde{p}(k)_{k=0}, \tag{89}$$

$$D_{ij} \equiv -\frac{1}{2} \tau_0^{-1} \frac{\partial^2}{\partial k_i k_j} \tilde{p}(k,s)_{k=0}. \tag{90}$$

The τ_0 denotes a typical transition time and is related to the transport dynamics and heterogeneity length scales. It will be specified below. The transport equation (85) then reduces to

$$s\overline{\overline{c}}^{*}(k,s) - \{iuk - kDk\}\frac{s\tau_0\psi^{*}(s)}{1-\psi^{*}(s)}\overline{\overline{c}}^{*}(k,s) = 1, \tag{91}$$

which is identical to the Laplace transform of (60) if we identify the memory function as

$$M^{*}(s) \equiv \frac{s\tau_0\psi^{*}(s)}{1-\psi^{*}(s)}. \tag{92}$$

Using (61) for $M^{*}(s)$ and identifying $\tau_0 \equiv \tau_u$, we obtain for the Laplace transform of the transition time distribution,

$$\psi^{*}(s) = \{1 + s\tau_u[1 + \varphi^{*}(s)]\}^{-1}. \tag{93}$$

Inserting the Laplace transform of (59) for $\varphi^{*}(s)$ yields expression (74) for the transition time distribution.

2. Power-law tails

Anomalous transport in CTRW is modeled by a transit time distribution exhibiting a power-law tail for large transit times, e.g., [42–44,62,63],

$$\psi(t) \propto t^{-1-\beta} \tag{94}$$

for $0<\beta<2$. We want to trace such behavior back and explicitly link it to the heterogeneity distribution. Thus we consider now a medium that is characterized by a broad distribution of retardation factors, which implies for the single variable distribution $P(r)$ of $r(x)$, see Sec. III B,

$$P(r) \propto \left(\frac{r}{r_1}\right)^{-1-\gamma} \tag{95}$$

for some r range, $r_1 \ll r \ll r_2$, and $0<\beta<2$. Inserting (95) into (74) and expanding for $r_2^{-1} \ll s\tau_u \ll r_1^{-1}$ yields for $N<\gamma<N+1$, see Appendix D,

$$\psi^{*}(s) = 1 + \sum_{j=1}^{N}(-1)^j a_j s^j + (-1)^{N+1} a_\gamma (s\tau_u r_1)^\gamma + \cdots, \tag{96}$$

where the dots denote subleading contributions, the a_j and a_γ are constants. The small-s expansion (96) implies the following behavior of $\psi(t)$, see Appendix D and, e.g., [42,53]:

$$\psi(t) \propto \left(\frac{t}{r_1\tau_u}\right)^{-1-\gamma} \tag{97}$$

for $\tau_u r_1 \ll t \ll \tau_u r_2$. This implies that in fact $\beta \equiv \gamma$, i.e., the power law in the heterogeneity distribution translates one to one to a power in the transit time distribution. It is not particularly surprising that a power-law tail in the heterogeneity distribution leads to anomalous transport behavior. This is in fact the phenomenological basis for many CTRW modeling approaches. The significance of the presented result lies in the fact that it provides an explicit and exact map of the disorder distribution on the transit time distribution and thus on effective transport.

V. SUMMARY AND CONCLUSIONS

We study effective transport in one spatial dimension under spatially varying linear instantaneous equilibrium adsorption properties, which are quantified in terms of a random retardation factor.

In a stochastic framework we derive formal effective transport equations for the mobile and total particle distributions, respectively, in Fourier-Laplace space. These effective equations are characterized by a spatiotemporal memory kernel, which is related to the self-energy $\Sigma(k,s)$. The latter plays a central role as it integrates the impact of medium heterogeneities on effective transport. The derivation of exact closed form expressions for $\Sigma(k,s)$ is complicated and in many cases only possible in the framework of a perturbation expansion in the fluctuations of the random retardation factor. For a short-range correlated random retardation factor, we determine an exact nonperturbative expression for the self-energy, which defines the effective reaction and transport dynamics.

The resulting effective transport equation for the mobile particle distribution quantifies the impact of spatial heterogeneities on effective transport and reaction dynamics. We find that the effective description of transport under spatially heterogeneous equilibrium adsorption reactions, is equivalent to transport under spatially homogeneous linear kinetic adsorption reactions. The distribution of adsorption times is given explicitly in terms of the disorder distribution.

Furthermore, we show that the effective transport equation for the total particle distribution describes a decoupled continuous time random walk. The explicit nature of the derived effective transport framework allows us to establish a direct map of the static disorder distribution on the transition time distribution, which provides a strong theoretical argument for the use of CTRW approaches to model effective transport in random environments.

ACKNOWLEDGMENTS

We are grateful to Andrea Cortis, Jesus Carrera, and Harvey Scher for stimulating discussions. M.D. gratefully acknowledges the financial support of the Spanish Secretaría de Estado de Educación y Universidades, the program "Ramon y Cajal" of the Spanish Ministry of Science and Technology, the Minerva Foundation of the Max-Planck Society, ENRESA (Empresa Nacional de Residuos Radioactivos) and the European Union IP FUNMIG (Contract No. 516514). B.B. gratefully acknowledges the support of the Israel Science Foundation (Grant No. 598/04).

APPENDIX A: INTEGRAL TRANSFORMS

The Laplace transform is defined by, e.g., [64],

$$\varphi^{*}(s) = \int_0^\infty dt\, \exp(-st)\varphi(t), \tag{A1}$$

$$\varphi(t) = \int_{\gamma-i\infty}^{\gamma+i\infty} ds\, \exp(st)\varphi^{*}(s). \tag{A2}$$

The γ is chosen so that singularities of $\varphi^{*}(s)$ lie to the left of the line $(\gamma-i\infty, \gamma+i\infty)$. Laplace transformed quantities are marked by an asterisk.

The Fourier transform here is defined by

$$\tilde{r}(k) = \int dx \exp(ikx) r(x), \tag{A3}$$

$$r(x) = \int \frac{dk}{(2\pi)} \exp(-ikx) \tilde{r}(k). \tag{A4}$$

Fourier transformed quantities are marked by a tilde.

APPENDIX B: ENSEMBLE AVERAGED CONCENTRATION

1. Green function

Consider the Laplace transform of our working equation (14):

$$s(1 + r(x)) g^*(x,s) + \left\{ u \frac{\partial}{\partial x} - D \frac{\partial^2}{\partial x^2} \right\} g^*(x,s) = \delta(x). \tag{B1}$$

The Green function $G(x,x',s)$ satisfies

$$s(1 + r(x)) G(x,x',s) + \left\{ u \frac{\partial}{\partial x} - D \frac{\partial^2}{\partial x^2} \right\} G(x,x',s) = \delta(x - x'), \tag{B2}$$

while the adjoint Green function $G^\dagger(x',x,s)$ solves

$$s(1 + r(x)) G^\dagger(x',x,s) - \left\{ u \frac{\partial}{\partial x} + D \frac{\partial^2}{\partial x^2} \right\} G^\dagger(x',x,s) = \delta(x - x'). \tag{B3}$$

According to the generalized Green theorem the following relation between the Green function and its adjoint holds [e.g., [65]],

$$G^\dagger(x',x,s) = G(x,x',s), \tag{B4}$$

and accordingly for the Fourier transformed functions,

$$\tilde{G}^\dagger(q,k,s) = \tilde{G}(k,q,s). \tag{B5}$$

The concentration distribution $g^*(x,s)$ is given by

$$g^*(x,s) = G(x,x' = 0,s) = G^\dagger(x' = 0,x,s), \tag{B6}$$

which reads in Fourier space as

$$\tilde{g}^*(k,s) = \int_q \tilde{G}(k,q,s) = \int_q \tilde{G}^\dagger(q,k,s). \tag{B7}$$

2. Ensemble averaged Green function

The random field $r(x)$ is assumed to be translation invariant. Using the (functional) probability distribution $\mathcal{P}(\{r(x)\})$ this property can be expressed by

$$\mathcal{P}(\{r(x)\}) = \mathcal{P}(\{r_L(x)\}), \tag{B8}$$

where $\mathcal{P}(\{r_L(x)\})$ denotes the joint distribution of $r_L(x) = r(x + L)$ with some constant translation L. For the following argumentation, we will denote the Green function for the shifted field r_L by $G_L(x,x',s)$ The translation invariance implies for the ensemble average of the Green function,

$$\overline{G(x,x',s)} = \overline{G_L(x,x',s)}. \tag{B9}$$

The shifted Green function $G_L(x,x',s)$ solves

$$s(1 + r_L) G_L(x,x',s) + \left\{ u \frac{\partial}{\partial x} - D \frac{\partial^2}{\partial x^2} \right\} G_L(x,x',s) = \delta(x - x'). \tag{B10}$$

The solution of the latter equation is $G(x+L,x'+L,s)$, which can be verified easily by shifting both spatial arguments in Eq. (B2) by the constant L. Thus we obtain

$$\overline{G(x,x',s)} = \overline{G_L(x,x',s)}$$
$$\overline{G(x + L,x' + L,s)} = \overline{g^*}(x - x',s), \tag{B11}$$

where we used (B6). The ensemble averaged Green function is a function of the distance between the injection point x' and the observation point x only. By relation (B4), we obtain correspondingly for the ensemble averaged adjoint Green function,

$$\overline{G^\dagger(x,x',s)} = \overline{G(x',x,s)} = \overline{g^*}(x' - x,s). \tag{B12}$$

and thus we obtain

$$\overline{G(x,x',s)} = \overline{G^\dagger(-x,-x',s)} = \overline{g^*}(x - x',s), \tag{B13}$$

which reads in Fourier-Laplace space as

$$\overline{\tilde{G}(k,q,s)} = \overline{\tilde{G}^\dagger(-k,-q,s)} = (2\pi)^d \delta(k + q) \overline{\tilde{g}^*}(k,s). \tag{B14}$$

3. Ensemble averaged concentration distribution

To derive expression (21) for the ensemble averaged concentration distribution, we start from the ensemble averaged Fourier transformed adjoint Green function. From the Fourier transform of (B3) we obtain an integral equation for $\tilde{G}^\dagger(k,q,s)$,

$$\tilde{G}^\dagger(k,q,s) = (2\pi)^d \delta(k + q) \tilde{g}_0^*(-k,s) - \tilde{g}_0^*(-k,s) s \times \int_{k'} \tilde{r}(k') \tilde{G}^\dagger(k - k',q,s). \tag{B15}$$

Taking the ensemble average of the latter equation yields

$$\overline{\tilde{G}^\dagger(k,q,s)} = (2\pi)^d \delta(k + q) \tilde{g}_0^*(-k,s) - \tilde{g}_0^*(-k,s) s \int_{k'} \overline{\tilde{r}(k') \tilde{G}^\dagger(k - k',q,s)}. \tag{B16}$$

Owing to relation (B14), the right side is proportional to $\delta(k+q)$, which implies in particular

$$s \int_{k'} \overline{\tilde{r}(k') \tilde{G}^\dagger(k - k',q,s)} \propto \delta(k + q). \tag{B17}$$

Hence, we can rewrite Eq. (B16) under the protection of the ensemble average by

$$\overline{\tilde{G}^{\dagger}(k,q,s)} = (2\pi)^d \delta(k+q)\tilde{g}_0^*(-k,s) - \tilde{g}_0^*(-k,s)s\int_{k'} \overline{\tilde{r}(k')\tilde{G}^{\dagger}(-q-k',-k,s)}. \tag{B18}$$

According to (B7) and (B14), $\overline{\tilde{g}^*}(k,s)$ is given by

$$\overline{\tilde{g}^*}(k,s) = \int_q \overline{\tilde{G}^{\dagger}(q,k,s)} = \int_q \overline{\tilde{G}^{\dagger}(-k,-q,s)}. \tag{B19}$$

Thus we obtain from (B18) and (B19),

$$\overline{\tilde{g}^*}(k,s) = \tilde{g}_0^*(k,s) - \tilde{g}_0^*(k,s)s\int_{k'} \overline{\tilde{r}(k')\tilde{g}^*(k,s)}. \tag{B20}$$

We insert now the right side of the integral equation (18) for $\tilde{g}^*(k,s)$ into the right side of (B20) and obtain (21). A corresponding relation was derived and used for transport in a random velocity field (e.g., [12,13]).

APPENDIX C: INVERSE LAPLACE TRANSFORM OF THE MEMORY FUNCTION

In order to perform the inverse Laplace transform of (57), we divide the r integration according to

$$\varphi^*(s) = \int_{-r_0}^{0} dr\, P(r)\frac{-|r|}{1-|r|s\tau_u} + \int_0^{\infty} dr\, P(r)\frac{r}{1+rs\tau_u}. \tag{C1}$$

Recall that $0<s\tau_u<1$ for the development of this expression. This implies that for the performance of the inverse Laplace transform, $0<\mathrm{Re}(s)<\tau_u^{-1}$, with a complex valued s. This means in particular that $0<\gamma<\tau_u^{-1}$ in (A2) for the inverse Laplace transform. The integrand of the first expression on the right has a pole at $(|r|\tau_u)^{-1}$, which is larger than τ_u^{-1} as $|r|$ is between 0 and r_0 and $r_0<1$. Thus the pole lies on the right of the line $(\gamma-i\infty,\gamma+i\infty)$ and the inverse Laplace transform of the first term on the right is zero.

The integrand of the second expression on the right has a pole at $-(r\tau_u)^{-1}$, which lies at the left of the line $(\gamma-i\infty,\gamma+i\infty)$. Thus the inverse Laplace transform of (57) is given by (59).

APPENDIX D: ASYMPTOTIC EXPANSION

To derive the small s expansion (96) for the Laplace transform of the transit time distribution, we start with (59) for the memory function $\varphi(t)$. Transforming the integration variable r according to $y=t/(r\tau_u)$, $\varphi(t)$ reads as

$$\varphi(t) = \tau_u^{-1}\int_0^{\infty} dy \frac{t}{y^2\tau_u} P\left(\frac{t}{y\tau_u}\right)\exp(-y). \tag{D1}$$

The Laplace transform of this expression is given by

$$\varphi^*(s) = -\tau_u^{-1}\int_0^{\infty} \frac{d}{ds} y^{-1}P^*(ys\tau_u)\exp(-y), \tag{D2}$$

with the Laplace transform of $P(r)$ given by

$$P^*(\mu) = \int_0^{\infty} dr\, P(r)\exp(-r\mu). \tag{D3}$$

For a $P(r)$ exhibiting the power-law behavior (95), $P^*(\mu)$ can be expanded for small $r_2^{-1} \ll \mu \ll r_1^{-1}$ according to, e.g., [42,53],

$$P^*(\mu) = \sum_{j=0}^{N} (-1)^j \alpha_j \mu^j + (-1)^{N+1}\alpha_\gamma r_1(\mu r_1)^\gamma + \cdots, \tag{D4}$$

for $N<\gamma<N+1$. The dots denote subleading contributions. The constants α_j $(j=1,2)$ and α_γ are given by

$$\alpha_j = \frac{1}{j!}\frac{d}{d\mu}P^*(\mu)_{\mu=0} \tag{D5}$$

$$\alpha_\gamma = \frac{C\Gamma(j+1-\gamma)\Gamma(\gamma-j)}{\Gamma(\gamma+1)}, \tag{D6}$$

with $\Gamma(\gamma)$ the Gamma function as defined in [66], C a proportionality constant. Inserting this small μ approximation into (D2) for the Laplace transform of the memory function, we obtain

$$\varphi^*(s) = \tau_u^{-1}\left\{\sum_{j=1}^{N}(-1)^j\alpha_j j\Gamma(j+1)s^{j-1} + (-1)^{N+1}\alpha_\gamma\gamma\Gamma(\gamma+1)r_1^2\tau_u(s\tau_u r_1)^{\gamma-1}\right\} + \cdots. \tag{D7}$$

Inserting this expansion for $\varphi^*(s)$ into (93) and expanding the resulting expression up to $(s\tau_u r_1)^\gamma$ yields the small s approximation (96) for $\psi^*(s)$. Expansion (96) is of the same type as (D4). Thus, $\psi(t)$ shows the same power-law behavior for a time regime given by $\tau_u r_1 \ll t \ll \tau_u r_2$, namely (97).

[1] J. Villermaux, J. Chromatogr. **406**, 11 (1987).
[2] A. Felinger, A. Cavazzini, and F. Dondi, J. Chromatogr., A **1043**, 149 (2004).
[3] M. Sardin, D. Schweich, F. J. Leij, and M. T. van Genuchten, Water Resour. Res. **27**, 2287 (1991).
[4] K. Roth and W. A. Jury, Water Resour. Res. **29**, 1195 (1993).
[5] D. T. Burr, E. Sudicky, and R. Naff, Water Resour. Res. **30**, 791 (1994).
[6] F. Miralles-Wilhelm and L. W. Gelhar, Water Resour. Res. **32**, 1541 (1996).
[7] J. Membrez, P. Infelta, and A. Renken, Chem. Eng. Sci. **51**, 4489 (1996).
[8] C. Calonder and P. Van Tassel, Langmuir **17**, 4392 (2001).
[9] G. Seisenberger, M. U. Ried, T. Endrebeta, H. Buning, M.

Hallek, and C. Brauchle, Science **294**, 1929 (2001).
[10] O. Taiwo and R. King, Chem. Eng. Process. **42**, 561 (2003).
[11] G. J. Szollosi, I. Derenyi, and J. Voros, Physica A **343**, 359 (2004).
[12] R. H. Kraichnan, J. Fluid Mech. **5**, 497 (1959).
[13] P. H. Roberts, J. Fluid Mech. **11**, 257 (1961).
[14] R. H. Kraichnan, Phys. Fluids **13**, 22 (1970).
[15] R. H. Kraichnan, J. Fluid Mech. **77**, 753 (1976).
[16] I. T. Drummond, S. Duane, and R. R. Horgan, J. Fluid Mech. **138**, 75 (1984).
[17] J. A. Aronovitz and D. R. Nelson, Phys. Rev. A **30**, 1948 (1983).
[18] D. S. Fisher, D. Friedan, Z. Qiu, S. J. Shenker, and S. H. Shenker, Phys. Rev. A **31**, 3841 (1985).
[19] L. W. Gelhar and C. L. Axness, Water Resour. Res. **19**, 161 (1983).
[20] D. L. Koch and J. F. Brady, J. Fluid Mech. **180**, 387 (1987).
[21] G. Dagan, Water Resour. Res. **24**, 1491 (1988).
[22] J. P. Bouchaud and A. Georges, Phys. Rep. **195**, 127 (1990).
[23] S. P. Neuman, Water Resour. Res. **29**, 633 (1993).
[24] M. W. Deem, Phys. Rev. E **51**, 4319 (1995).
[25] D. S. Dean, I. T. Drummond, and R. R. Horgan, Phys. Rev. E **63**, 061205 (2001).
[26] B. X. Hu, F.-W. Deng, and J. H. Cushman, Water Resour. Res. **31**, 2239 (1995).
[27] H. Rajaram, Adv. Water Resour. **20**, 217 (1997).
[28] P. C. Lichtner and D. M. Tartakovsky, Stochastic Environ. Res. and Risk Assessment **17**, 419 (2003).
[29] J. Cushman, Water Resour. Res. **27**, 643 (1991).
[30] D. L. Koch and E. S. G. Shaqfeh, Phys. Fluids A **4**, 887 (1992).
[31] F.-W. Deng, J. H. Cushman, and J. W. Delleur, Water Resour. Res. **29**, 3241 (1993).
[32] J. H. Cushman, X. Hu, and T. R. Ginn, J. Stat. Phys. **75**, 859 (1994).
[33] J. H. Cushman, B. X. Hu, and F.-W. Deng, Water Resour. Res. **31**, 2219 (1995).
[34] M. S. Green, J. Chem. Phys. **20**, 1281 (1952).
[35] R. Kubo, J. Phys. Soc. Jpn. **12**, 570 (1957).
[36] H. Mori, Phys. Rev. **112**, 1829 (1958).
[37] R. Zwanzig, Phys. Rev. **129**, 486 (1963).
[38] R. Zwanzig, Phys. Rev. **124**, 983 (1961).
[39] E. W. Montroll and G. H. Weiss, J. Math. Phys. **6**, 167 (1965).
[40] H. Scher and M. Lax, Phys. Rev. B **7**, 4491 (1973).
[41] H. Scher and M. Lax, Phys. Rev. B **7**, 4502 (1973).
[42] H. Scher and E. W. Montroll, Phys. Rev. B **12**, 2455 (1975).
[43] B. Berkowitz and H. Scher, Phys. Rev. Lett. **79**, 4038 (1997).
[44] B. Berkowitz and H. Scher, Phys. Rev. E **57**, 5858 (1998).
[45] F. W. Schmidlin, Phys. Rev. B **16**, 2362 (1977).
[46] R. Metzler and J. Klafter, Phys. Rep. **339**, 1 (2000).
[47] J. Bisquert, Phys. Rev. Lett. **91**, 010602 (2003).
[48] J. Klafter and R. Silbey, Phys. Rev. Lett. **44**, 55 (1980).
[49] B. Berkowitz and H. Scher, Water Resour. Res. **31**, 1461 (1995).
[50] Y. Hatano and N. Hatano, Water Resour. Res. **34**, 1027 (1998).
[51] B. Berkowitz, G. Kosakowski, G. Margolin, and H. Scher, Ground Water **39**, 593 (2001).
[52] B. Berkowitz, J. Klafter, R. Metzler, and H. Scher, Water Resour. Res. **38**, 1191 (2002).
[53] M. Dentz and B. Berkowitz, Water Resour. Res. **39**, 1111 (2003).
[54] M. Dentz, A. Cortis, H. Scher, and B. Berkowitz, Adv. Water Resour. **27**, 155 (2004).
[55] G. Pfister and H. Scher, Adv. Phys. **27**, 747 (1978).
[56] C. F. Harvey and S. M. Gorelick, Water Resour. Res. **31**, 1895 (1995).
[57] R. Haggerty and S. M. Gorelick, Water Resour. Res. **31**, 2383 (1995).
[58] J. Carrera, X. Sánchez-Vila, I. Benet, A. Medina, G. Galarza, and J. Guimerà, Hydrogeol. J. **6**, 178 (1998).
[59] R. Haggerty, S. A. McKenna, and L. C. Meigs, Water Resour. Res. **36**, 3467 (2000).
[60] S. Grabtchak and M. Cocivera, Phys. Rev. B **58**, 12594 (1998).
[61] H. Risken, *The Fokker-Planck Equation: Methods of Solution and Applications*, 2nd ed., Springer Series in Synergetics Vol. 18 (Springer, Berlin, 1989).
[62] G. Margolin and B. Berkowitz, J. Phys. Chem. B **104**, 3942 (2000).
[63] G. Margolin and B. Berkowitz, Phys. Rev. E **65**, 031101 (2002).
[64] H. S. Carslaw and J. C. Jaeger, *Conduction of Heat in Solids* (Oxford University Press, New York, 1959).
[65] P. Morse and H. Feshbach, *Methods of Theoretical Physics* (McGraw-Hill, New York, 1953).
[66] M. Abramowitz and I. A. Stegun, *Handbook of Mathematical Functions* (Dover, New York, 1972).